EFFECT OF SOIL-STRUCTURE INTERACTION ON PERFORMACE BASED DESIGN OF INTEGRAL ABUTMENT BRIDGES

Kianosh Ashkani Zadeh,
PhD Student, The University of British Columbia, Vancouver, Canada
kianosh@civil.ubc.ca

Carlos E. Ventura
Professor, The University of British Columbia, Vancouver, Canada
ventura@civil.ubc.ca

ABSTRACT: The effect of soil-structure interaction on the behaviour of integral abutment bridges is studied within the framework of performance-based earthquake engineering. Non-linear incremental dynamic analysis (IDA) is employed to develop the fragility curves for non-SSI and SSI models. For this purpose, three different types of integral abutment bridges are modeled in detail with and without SSI features. 20 well-selected ground motions were used in the IDA of bridge models. Relative displacement and drift of the abutment back walls and pier columns are considered as engineering demand parameters (EDPs) and spectral acceleration of ground motions is chosen as the Intensity Measure (IM). Collapse Margin Ratio (*CMR*), which is a characteristic measure of collapse safety of the structure, is chosen to objectively compare the response of non-SSI and SSI models. It is shown in this study that considering the soil-structure interaction has led to a significant decrease in the collapse margin ratio when compared to non-SSI models. This indicates that ignoring the soil effect may result in under estimation of probability of collapse.

1. Introduction

Strong earthquake shaking has resulted in collapse of several pile bridges worldwide. Lack of understanding and consideration of the effect of Soil-Structure Interaction (SSI) is among the major reasons behind these devastating collapses. As discussed in Mitchell et al. (1995) and Mylonakis et al. (1997), several bridge piers are damaged due to soil-pile-bridge seismic interaction during the Northridge Earthquake in 1994. In addition, SSI had a major contribution to the collapse of the 630-meter long Hanshin Expressway Bridge during the Kobe Earthquake in 1995. An analytical study of the Hanshin Expressway showed that soil characteristics had a significant effect on the behaviour of this structure. Modification of earthquake frequency content due to soft soil resulted in intensifying the structural response. Moreover, the soft soil resulted in elongation of the fundamental period of the structure causing a more severe response of the bridge, rather than a lesser response. Another example where SSI had a major contribution to structural failure is the collapse of the Cypress Structure in Oakland during the Loma Prieta earthquake in 1989 (Barbosa et al., 2014). The loose sand that the structure was built on, led to a more severe response by the structure which ultimately resulted in structural collapse of many sections of this bridge.

Current seismic design codes are lacking comprehensive requirements to deal with SSI effects. The effect of soft soil on the response spectrum is incorporated in via the Fα and Fv site response coefficients. But to minimize seismic risk and avoid catastrophic failure of bridges, change in the structural response due to soil-structure interaction needs to be effectively addressed in the next generation of bridge design codes. This is especially important for regions with soft soil and high earthquake risk. In addition, one of the important aspects missing in the current code is the effect of different earthquake types, specifically subduction zone earthquakes (Barbosa et al., 2014).

In this study, and within a performance-based design framework, the Incremental Dynamic Analysis (IDA) method is employed to investigate the effect of soil-structure interaction on the potential collapse of integral abutment bridges. The concept of Collapse Marginal Ratios (*CMR*) introduced by FEMA P-695 (FEMA, 2009) as a collapse measure for buildings is adapted here to bridge structures. This concept is used in this study to compare the performance of SSI and non-SSI models. Further information on the methodology and approach used for the study conducted by the authors can be found in Ashkani Zadeh (2013).

2. Methodology

The proposed methodology consists of three steps: Step1: Model construction and analysis; Step 2: Calculation of probability of collapse; and Step 3: Interpretation and comparison of collapse margin ratios. As the first step, detailed models of the bridges are constructed. An incremental dynamic analysis is performed using a set of selected ground motions. Outcomes of the IDA are interpreted as probability of collapse, and the fragility curves constructed based on these results are used to calculate the collapse margin ratios (*CMR*). A schematic of the methodology adopted here is presented in Fig.1.

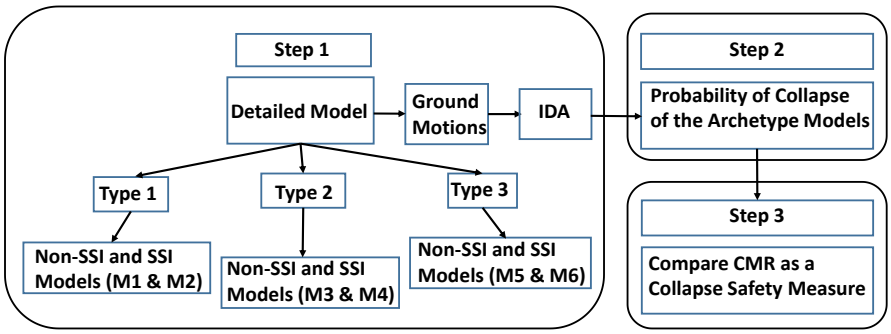

Fig. 1 – General framework of the study research

2.1 Model Construction and Analysis (Step 1)

This step includes the construction of a finite element model (FE) of a bridge prototype, selection of a suitable set of ground motions and implementation of the IDA using the FE model and the ground motions. Some details for each step are discussed below.

2.1a FE Model construction

3-D nonlinear models of various types of integral abutment bridges are constructed using computer program SeismoStruct (SesimoSoft, 2013). SeismoStruct is capable of performing non-linear dynamic analysis. The non-linear behaviour of structural components as well as geometric nonlinearities are simulated by this software.

For each bridge, two archetype models are defined: One considering soil-structure interaction and another without the SSI effects. The effect of soil-structure interaction from soils supporting the piles and abutment backwalls are simulated. The SSI p-y link introduced by (Allotey and El Naggar, 2008) is employed here. The properties of soil sub-layer models are considered in determining the link properties. The effect of the soil behind the abutment backwall is simulated using springs as recommend by the CALTRANS guidelines (CALTRANS, 2013).

A nonlinear soil-structure interaction analysis based on Winkler-spring model developed by El Negar and co-workers (Allotey et al., 2008) is performed to determine the soil effect around the piles. Features such as loading and unloading rules, modeling of radiation damping and cyclic degradation, and slack zone for the analysis of shallow and deep foundation are considered in this model. This approach is incorporated in various analysis software, including SeismoStruct. Schematic views of the loading and unloading curves of this model are shown in Fig. 2. The recommendations provided by the API code (API, 2005) (clay layers) and L-Pile manual (Resee et al., 2004) (sand layer) are adapted to calculate the p-y curves for each layer.

2.1b Ground motions

To address ground motion uncertainty, a set of 20 selected ground motions from the PEER Strong Motion database is chosen to perform nonlinear response history analysis. The approach recommended by FEMA P-695 (FEMA P-695, 2009) is employed here to select the ground motions. In this approach, ground motions with response spectrum that best fits to mean site spectrum calculated based on hazard analysis are chosen. Minimizing the differences between the two spectra at the fundamental period to account for spectral shape effect is the main objective here (Baker, 2005). This approach is used to include ground motion spectra shape characteristics to ensure an unbiased estimate of the collapse probabilities. Here,

epsilon (ε) is defined as number of standard deviations by which an observed logarithmic spectral acceleration differs from the mean logarithmic spectral acceleration of a ground-motion prediction values at the fundamental period of the structures. Hazard spectra for the five selected motion and the target spectrum along with the period of interest are shown in Fig. 3.

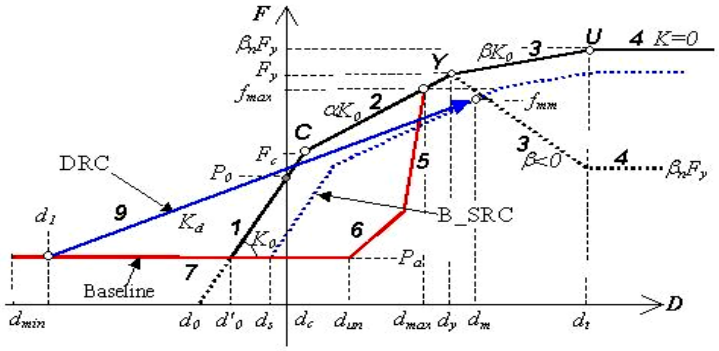

Fig. 2 – Backbone curve of the Winkler model used in the SSI p-y links - Source: (SeismoSoft, 2014)

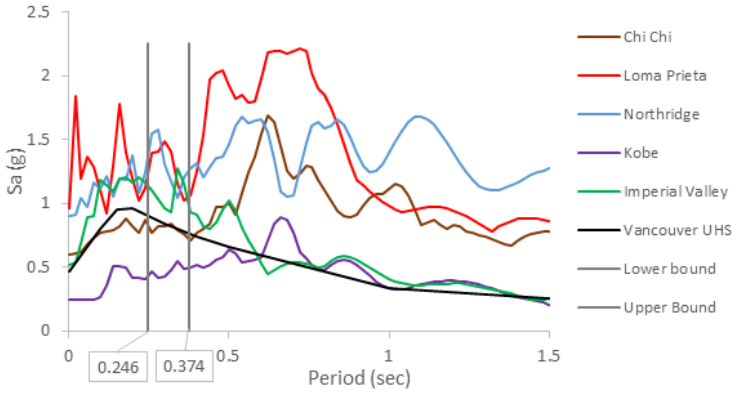

Fig. 3 – Ground motion spectra along with the target spectrum, and the range of period of interest

2.1c Incremental Dynamic Analysis (IDA)

In IDA the structure is subjected to a sequence of acceleration time-histories of increasing intensity until it reaches a predetermined performance point, such as a collapse point. This approach is used to determine the median collapse intensity (Vamvatsikos and Cornell, 2002). Collapse conditions and the collapse fragility curves for each archetype model are predicted using a cumulative distribution function (CDF).

The analysis is performed using the selected earthquake time histories. An initial and incremental coefficient of 0.25 is employed in the IDA analysis presented here. In addition, acceleration time histories are applied in both X and Y directions (along and perpendicular to the bridge decks) to the nodes that were restrained in all directions.

Relative displacement and drifts of the abutment backwalls and pier columns are considered as engineering demand parameters (EDPs). Spectral acceleration is chosen as the intensity measure (IM).

Performance levels are evaluated based on ‘collapse prevention’ according to FEMA P-695. Therefore, the main focus is on the performance of seismic-force resisting system. In this study, actual collapse is not simulated explicitly; instead, non-simulated collapse modes are evaluated using limit state checks on structural response quantities calculated in the analyses (performance criteria).

In non-simulated collapse modes, failure of the first primary structural component is assumed as an indicator of structural collapse. As discussed in FEMA P-695, non-simulated limit state checks may result in lower estimates of the median collapse compared to the case that all the local failure modes are directly simulated (FEMA P-695, 2009).

2.2. Probability of Collapse (Step 2)

Outcomes of the incremental dynamic analysis can be presented as a fragility curve which shows probability of collapse as a function of spectral acceleration (S_a). A log-normal cumulative distribution function is then fitted to the point cloud of data using least square method as proposed by Baker (2015). The approach can be used for fitting fragility functions for a variety of situations, especially, collapse fragility functions obtained from structural analysis data assuming that collapse of a given structure are lognormally distributed. In this approach, a CDF can be fitted to IDA data, to provide a continuous estimate of the probability of collapse as a function of S_a using the following formula:

$$P(C \mid S_a = x) = \Phi\left(\frac{\ln(x/\mu)}{\sigma}\right) \quad (1)$$

in which,

$P(C \mid S_a = x)$ is the probability that a ground motion with $S_a = x$ will cause the structure to collapse,

$\Phi(\ )$ is the standard normal cumulative distribution function (CDF),

μ is the median of the fragility function (the S_a level with 50% probability of collapse)

and σ is the standard deviation of $\ln S_a$ or dispersion of S_a.

2.3. Collapse Marginal Ratio (*CMR*) (Step 3)

Collapse Margin Ratio (*CMR*) is the primary parameter used to characterize the safety against collapse of the structures being investigated. *CMR* is defined as the ratio between the median collapse intensity (S_{CT}) and the Maximum Considered Event (MCE) intensity (S_{MT}). MCE intensity (S_{MT}) is obtained from the response spectrum of MCE ground motions at the fundamental period, T_1 (FEMA P-695, 2009). *CMR* is calculated as per Eq. 2 below.

$$CMR = S_{CT} / S_{MT}(T_1) \quad (2)$$

The CMR parameter offers an objective measure for the structural collapse. This parameter combines the fragility curve with the site-specific response spectrum. Higher *CMR* values indicate less chance of failure while cases with lower *CMR* values have a higher probability of failure.

3. Bridge Models

In this section a brief discussion of the bridge models selected for this study is provided. Details of how the SSI effects have been incorporated into these models are also presented.

3.1. Archetype Models

To determine and compare the probability of collapse of the integral abutment bridges three different types of bridges are considered (see Table 1 for details). For each bridge type, two archetype models are defined: One considering soil-structure interaction and another without the SSI effects. Therefore, a total six multi-degree of freedom (MDOF) models have been developed (M1-M6 as shown in Fig. 4 and Table 1).

M1 is a simplified model of a single span integral abutment bridge with 30° skew angle. M2 is the SSI version of M1 considering the effect of the soil around the abutment piles assuming a soil sub-layer arrangement along the piles. This effect is simulated by employing SSI p-y links corresponding to each layer of soil as discussed in section 2.1.

M3 is a simplified MDOF model of a three span integral abutment bridge with a 15° skew angle. M4 is the SSI version of M3 considering the effect of the soil behind the abutment backwalls using CALTRANS springs and soil around the abutment and pier piles assuming the same soil sub-layer arrangement and the SSI p-y links along the piles as used in M2.

Finally, M5 is a simplified model of a two-band common semi-integral abutment bridge with 3 spans and a 6° skew angle. M6 is the SSI version of M5 considering the effect of the soil behind the abutment backwalls using CALTRANS springs. Diagrams of the bridge types are shown in Fig. 4.

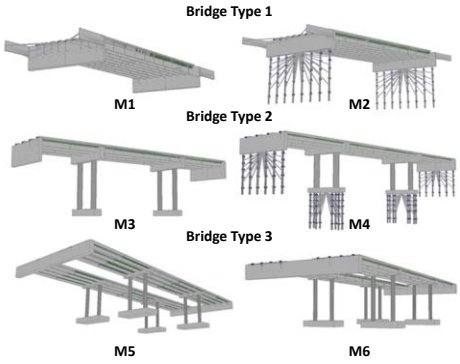

Fig. 4 – Shows different three type of bridges used in this study

Features of the above bridge models are summarized in Table 1 and the constructed prototype models are presented in Fig. 5.

Table 1 – Summary of the bridge types and archetype models are developed and used in this study

Archetype Model	Structural Feature	Span Length (m)	Skewness Angle (°)	Horizontal Radius (m)	SSI Feature
M2	Integral abutment bridge with abutment pile foundations and total 9 pre-stressed precast girders	38	30°	-	CALTRANS springs and SSI p-y links
M4	Integral abutment bridge with pier & abutment pile foundations and total 4 pre-stressed precast girders	17-29-19	15°	1009.95	CALTRANS springs and SSI p-y links
M6	Two-band semi-Integral abutment bridge with common seat abutment, pier pilecap deep foundation, intermediate diaphragm, and total 8 pre-stressed precast girders	27.5-37.5-27.5	6°	-	CALTRANS springs

3.2. SSI model parameters

To account for soil effect around the abutment and pier piles, the following soil sub-layer arrangement is considered. The sub-soil layer arrangement is shown in Fig. 5.

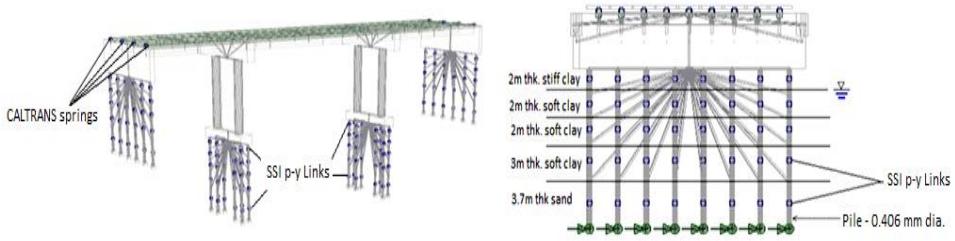

Fig. 5 – Shows assumed soil sub-layer around the piles and location of the assigned CALTRANS springs and SSI p-y links in the SSI models

The sub-layer arrangement is based on a geotechnical recommendation report provided by the Hatch Mott MacDonald and MMM Group (H5M joint venture) for the design stage of one of the newly constructed bridges as a part of the PORT MANN Highway 1 Project in Vancouver (Hall, 2009).

The API code is used to develop the p-y curves for soft and stiff clay layers. The approach incorporated in computer program L-Pile is employed here to calculate the p-y curve for the sand layer. The resulting curves are presented in Fig 6. The parameters used in SeismoStruct are extracted from the p-y curves. Parameters of the tri-linear backbone p-y curves for each layer are presented in Table 2.

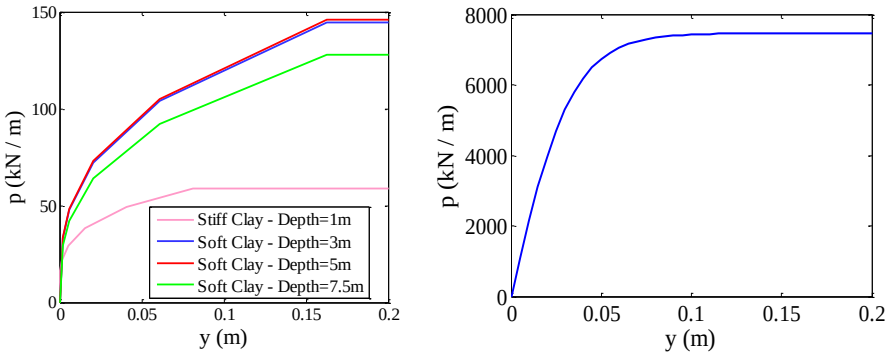

Fig. 6 – (a) Developed p-y curves based on the assumed sub-layers of soil surrounding piles using API code. (b) Obtained p-y curve for sand layer around the piles using L-Pile Manual.

For simplicity, soil layers around the abutment and pier piles are considered to be identical in M2 and M4 models.

Table 2 – Calculated parameters which obtained fitting a tri-linear curve to the derived p-y curves

Layer	Thickness (m)	Depth (m)	k_0 (kN/m)	α	β	P_u (kN)	F_y (kN)	$\beta_n=P_u/F_y$	F_c/F_y
Stiff Clay	2	1	11490.6	0.0969	0.040	117.2	98.6	1.189	0.595
Soft Clay	2	3	15651.5	0.1313	0.051	289.3	208.3	1.389	0.458
Soft Clay	2	5	15814.1	0.1313	0.051	292.3	210.5	1.389	0.458
Soft Clay	3	7.5	20756.1	0.1313	0.051	383.7	276.2	1.389	0.458
Silty Sand	3.7	10.85	685185.2	0.3484	0.060	27624.2	25900	1.067	0.714

in which,
k_0 : initial stiffness
α: second segment coefficient of stiffness of the nonlinear dynamic soil structure interaction model illustrated in Fig. 2.
β: stiffness ratio parameter in the SSI model which defines the stiffness of the third segment in proportion to k_0
P_u: soil ultimate strength
Fc: soil strength ratio at first turning point
Fy: soil yield strength
βn: strength ratio parameter in the SSI model

In this study, to account for the resistance due to the backfill passive pressure at the bridge abutments CALTRANS springs are attached to the abutment backwalls in the M2, M4 and M6 models. Stiffness of the abutment due to passive pressure of backfilling behind it is obtained based on section 7.8.1-2 SDC 2013 (CALTRANS, 2013) as per Eq. 3 and summarized in Table 3.

$$k_{abut} = k_i w\left(\frac{h}{1.7\text{m}}\right) \tag{3}$$

where, k_i is the initial stiffness of the embankment fill material behind the abutments, and based on section 7.81-1 of SDC 2013 can be calculated using Eq. 4:

$$k_i \approx \frac{28.7\ \text{kN/mm}}{\text{m}} \tag{4}$$

in which,

w is the projected width of the backwall or diaphragm for seat and diaphragm abutments respectively

h is the effective height of abutment which is determined based on the diaphragm design.

In this study, effective height is chosen considering the abutment diaphragms are designed for full soil pressure

Table 3 – Summary of calculated stiffness of the bridge abutments due to the embankment passive pressure force resisting movement

Models	k_i (kN/mm/m)	w (m)	h (m)	k_{abut} kN/mm)
M2	28.7	19.2	4.33	1404
M4	28.7	13.69	5.1	1178.54
M6	28.7	34.88	4	2355.43

4. Results

In this section the most important results of the implementation of the proposed methodology are presented. The IDA results are presented first, followed by a discussion of results from the comparisons of the CMR analyses.

4.1. IDA Results

The maximum pier column relative displacement graphs for all models predicted using the IDA were generated. The one for model M4 is presented in Fig. 7. To compare pier column drift ratios of the bridge models, hysteretic loops for one of their pier columns are plotted at the collapse stage. Figure 8 shows the pier column total drift ratio of the M3 and M4 models versus total base shear and moment for the Chi Chi ground motion. The M3 curve corresponds to time-history scale factor of 2.0 and the M4 model corresponds to scale factor of 0.75.

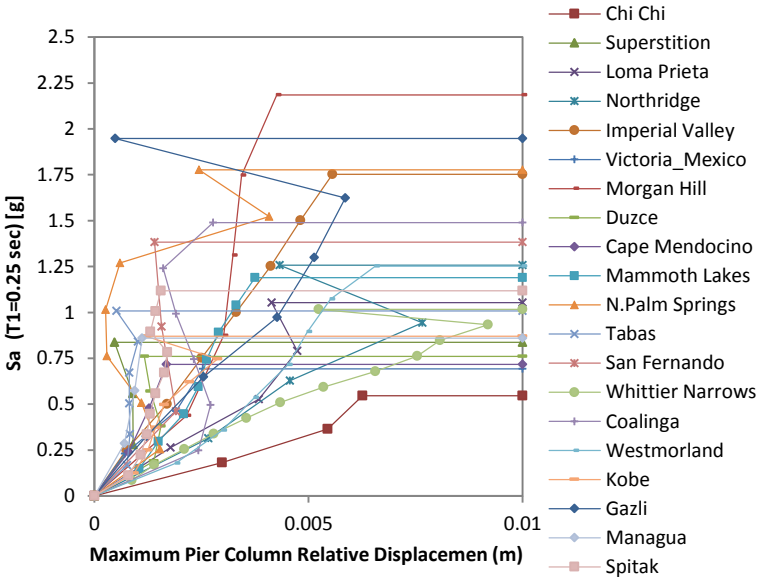

Fig. 7. Predicted pier column actual relative displacement along the bridge deck for M4 model.

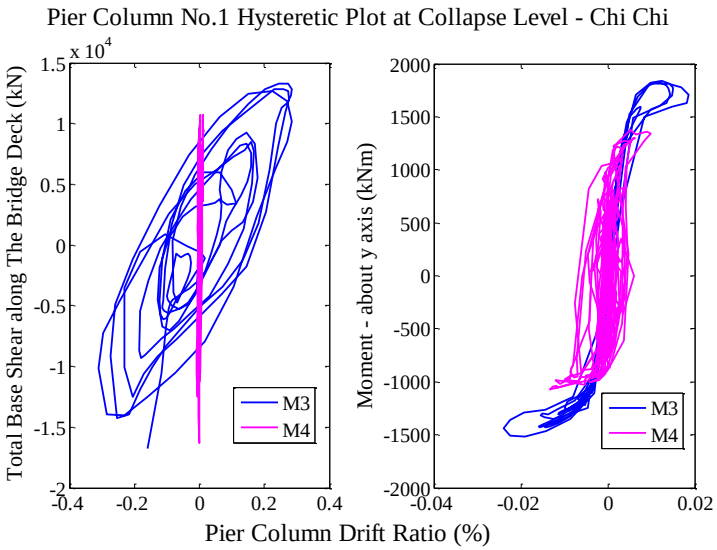

Fig. 8 – Pier column actual drift ratio across the bridge deck versus (a) total base shear, and (b) total moment calculated using IDA - M3 and M4 models.

It can be seen that column's drift for the SSI model (M4 model) is significantly reduced at the collapse level.

4.2. Probability of Collapse and Collapse Marginal Ratio (*CMR*) Results

Calculated probability of collapse of the archetype models are presented in Fig. 9. Assuming that shear wave velocity of the top 30m of the site sub-layer soil is between 360m/s and 750m/s, which is equivalent to soil site class C based on (NBCC, 2010), collapse margin ratios for 10%, 20%, and 50% (median) were calculated and the results are presented in Table 4.

Although pier drifts predicted in the SSI models (as shown in Fig. 8) are typically smaller than the corresponding non-SSI models, redistribution of load to other components, like the abutment, has led to earlier structural failure. This has consequently resulted in shifting the *CMR* curve corresponding to SSI models to the left when compared with the non-SSI counterparts.

As shown in Fig. 10, the SSI model shows a reduction in *CMR* values. As a result, for a given S_a, probability of collapse is increased.

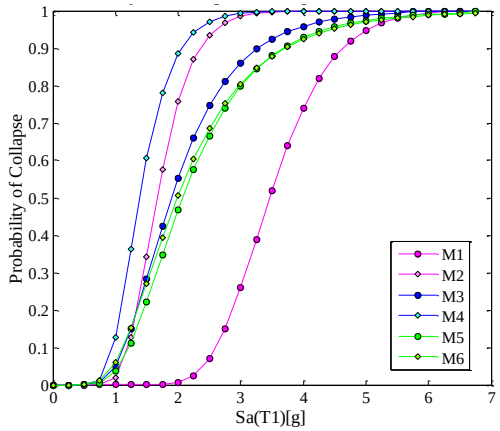

Fig. 9 – Calculated probability of collapse for all the archetype models

The effect of soil has led to change in the response of the structure leading to a re-distribution of loads in some members. On average, this has led to collapse of SSI models at smaller S_a levels, leading to a reduction in predicted *CMR* values. As an example, the M3 model subjected to the Chi Chi earthquake

fails at a S_a, level of 1.61g due to shear force in the abutments, whereas the SSI model of the same bridge (M4 model) has failed at S_a, of 0.54g due to Abutment concrete confinement strain and steel strain. See (Ashkani Zadeh, 2013) for further details.

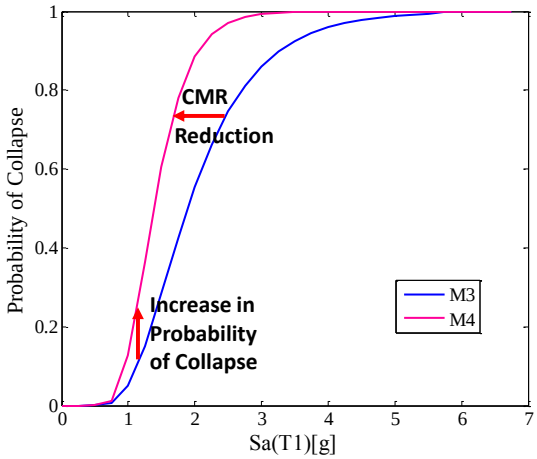

Fig. 10 – Reduction of *CMR* and increase of Probability of Collapse in SSI model

Table 4 – Summary of the calculated collapse margin ratios for median (50%), 10%, and 20% and for all models

Model	T_1 (sec)	$S_{ct\ 10\%}$ (g)	$S_{ct\ 20\%}$ (g)	$S_{ct\ @\ Median}$ (g)	$S_{MT\ @\ T1}$ (g)	$CMR_{10\%}$	$CMR_{20\%}$	CMR_{Median}
M1	0.25	2.59	2.86	3.46	0.90	2.88	3.18	3.84
M2	0.28	1.19	1.33	1.67	0.86	1.39	1.56	1.95
M3	0.34	1.13	1.34	1.90	0.80	1.41	1.68	2.38
M4	0.37	0.94	1.08	1.39	0.76	1.24	1.42	1.84
M5	0.37	1.21	1.45	2.08	0.76	1.60	1.91	2.74
M6	0.37	1.11	1.35	1.99	0.76	1.46	1.78	2.62

5. Conclusions

In this study, Incremental Dynamic Analysis (IDA) was employed to simulate the behavior of three bridge models. In all cases, the analyses were carried out with and without considering the SSI effects. A set of 20 selected ground motions was chosen for the IDA analysis. Non-simulated collapse mode was adopted as a collapse indicator. Fragility curves were fitted to predictions of IDA simulations for both non-SSI and SSI models. The concept of collapse margin ratio (*CMR*) was employed here to objectively compare the performance of these models. It was shown that the SSI models collapsed at lower S_a levels. As a result the collapse margin ratio values for the SSI models were smaller than the non-SSI counterparts.

This has led to a shift of fragility curves to the left side going from non-SSI to SSI models. This study shows that for the soil condition considered here neglecting the soil-structure interaction leads to under predicting the probability of collapse and results in a non-conservative design.

Acknowledgements

The authors would like to thank Natural Sciences and Engineering Research Council of Canada (NSERC) for the support for this study. The authors are indebted to Mr. Don Kennedy, P.Eng, and Mr. Alfred Kao, P.Eng. of Associated Engineering for providing helpful bridge documents and drawings.

References

API, A. P. (2005). Soil Reaction for Laterally Loaded Piles. in API Recommended Practice 2a-WSD (RP 2A-WSD) (pp. 68-71). Washington, D.C.: API Publishing Services.

ALLOTEY, Nii, EL NAGGAR, Hesham. (2008). Generalized dynamic Winkler model for nonlinear soil-structure interaction analysis. Can.Geotech, 560-573.

ASHKANI ZADEH, Kianosh. Seismic Analysis of the RC integral bridges using performance-based design approach including soil structure interaction. Vancouver: The University of British Columbia, 2013. https://circle.ubc.ca/handle/2429/45407.

BAKER, Jack, CORNELL, Allin. (2005). Vector Valued Ground Motion Intensity Measures for Probabilistic Analysis. PhD Theses, Stanford University, Civil and Environmental Engineering, Stanford.

BAKER, J.W. (2014). Efficient analytical fragility function fitting using dynamic structural analysis. In press.

BAKER, J.W. (2013). Research- Software and data-Tools for fragility function fitting. Retrieved June 10, 2013, from Baker Research Group: http://www.stanford.edu/~bakerjw/fragility.html

BARBOSA, Andre, MASON, Benjamin, and ROMNEY, Kyle. *SSI-Bridge: Soil-Bridge Interaction during Long-Duration Earthquake Motions*. Final Project Report. Corvallis: Pacific Northwest Transportation Consortium (PacTrans), 2014.

CALTRANS, C. D. (2013). Abutments- Longitudinal Abutment Response. In C. D. (Caltrans), Caltrans Seismic Design Criteria - VERSION 1.7 (pp. 7-51, 7-52). Sacramento, California: CALTRANS.

FEMA P-695 (2009). In U. D. Security, Quantification of Building Seismic Performance Factors (pp. 6-12). Washington, D.C.: FEDERAL EMERGENCY MANAGEMENT AGENCY.

HALL, Brian (2009). Geotechnical Memorandum for Leoran Brook Bridge No B5930 PMH1 Segment F1. Vancouver: Kiewit FLATIRON.

MITCHELL, Denis, BRUNEAU, Michel, WILLIAMS, Martin, ANDERSON, Donald, SAATCIOGLU, Murat, and SEXMITH, Robert. "Performance of bridges in the 1994 Northridge earthquake." *Can. J. Civ. Eng.* 22 (1995).

MYLONAKIS, George, NIKOLAOU, Aspasia, and GAZETAS, George. "Soil-Pile-Bridge Seismic Interaction: Kinematic and Inertial Effects. Part I: Soft Soil." *Earthquake Engineering and Structural Dynamics* (1997): VOL. 26, 337-359.

MYLONAKIS, George and GAZETAS, George. "Seismic Soil-Structure Interaction: Beneficial or Detrimental?" *Journal of Earthquake Engineering* Vol. 4, No. 3 (2000): 277-301.

MYLONAKIS, George (2000). The Role of Soil on the Collapse of 18 Piers of the Hanshin Expressway in the Kobe Earthquake. 12WCEE, 7.

SEISMOSOFT. (2014). SeismoStruct User manual for Version 7. Pavia-Italy: Seismosoft Ltd.

VAMVATSIKOS, Dimitrios, CORNELL, Allin (2002). Direct estimation of the seismic demand and capacity of MDOF systems through Incremental Dynamic Analysis of an SDOF approximation. 12th European Conference on Earthquake Engineering. London: 12th European Conference on Earthquake Engineering.